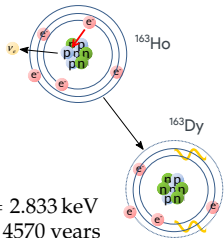
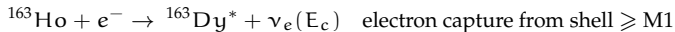


An overview of the status of HOLMES, an experiment for measuring the neutrino mass

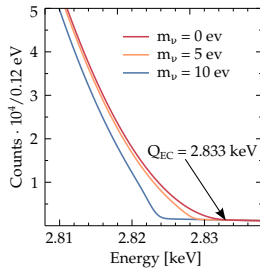
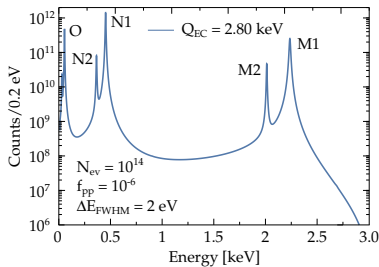
Elena Ferri

*University of Milano-Bicocca and INFN of Milano-Bicocca
on behalf of HOLMES collaboration*





$Q_{\text{EC}} = 2.833 \text{ keV}$
 $\tau_{1/2} \simeq 4570 \text{ years}$



- Calorimetric measurement of Dy atomic de-excitations (mostly non-radiative)

⇒ measurement of the entire energy released except the ν energy

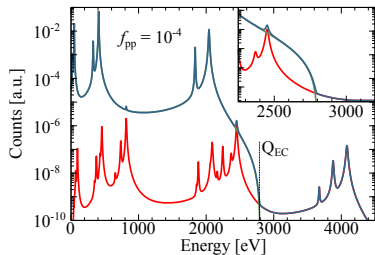
- rate at the end point depends on $(Q - E_{M1})$: the proximity to M1 resonance peak enhances the statistics at the end point (i.e. sensitivity on m_ν)

- Searching for a tiny deformation caused by a non-zero neutrino mass to the spectrum near its end point

proposed for the first time
 by A. De Rujula e M. Lusignoli in 1982
 Phys. Lett. 118B (1982) 429
 Nucl. Phys. B219 (1983) 277-301



$$S(E_c) = [N_{ev}(N_{EC}(E_c, m_v) + f_{pp} \times N_{EC}(E_c, 0) \otimes N_{EC}(E_c, 0)) + B(E_c)] \otimes R_{\Delta E}(E_c)$$



N_{ev}	: total number of events
$N_{EC}(E_c, m_v)$: ^{163}Ho spectrum
$B(E)$: background energy spectrum
$R_{\Delta E}(E_c)$: detector energy response function
f_{pp}	: fraction of pile-up events
$R_{\Delta E}(E_c)$: detector energy response function
ΔE	: interval of energy

more details on

[Eur. Phys. J. C 74 \(2014\) 3161](#)

- Pulse pile-up occurs when multiple events arrive within the temporal resolving time of the detector
- Unresolved pile-up events close to the end-point impairing effect on the end-point measurement
- The ^{163}Ho pile-up events spectrum is quite complex and presents a number of peaks at the end-point
- To resolve pile-up:
 - Detector with fast signal rise-time τ_{rise}
 - Pile-up recognition algorithm (i.e. Wiener filter, Singular Value Decomposition)



The m_ν statistical sensitivity has:

- **Strong** dependence on statistic: $\Sigma(m_\nu) \propto N_{\text{events}}^{1/4}$
- **Strong** dependence on pile-up: $f_{\text{pp}} \simeq A_{\text{EC}} \cdot \tau_{\text{res}}$
(A_{EC} : pixel activity, τ_{res} : time resolution)
- **Weak** dependence on energy resolution ΔE ;

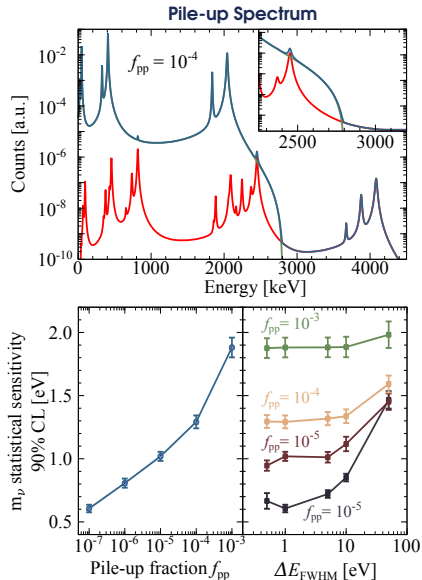
Multiplexable detectors with fast response are required

HOLMES

Neutrino mass determination with a sensitivity as low as ≈ 1 eV

- Microcalorimeters based on Transition Edge Sensors with ^{163}Ho implanted Au absorber
- Pixel activity of $A_{\text{EC}} \sim 300$ Bq/det
- Energy resolution: $\mathcal{O}(\text{eV})$
- Time resolution: $\tau_{\text{res}} \sim 3 \mu\text{s}$ ($\tau_{\text{rise}} = 10 - 20 \mu\text{s}$);
- 1000 channels for $3 \cdot 10^{13}$ events collected in $T_M = 3$ years

more details on
[Eur. Phys. J. C \(2015\) 75: 112](#)

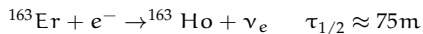
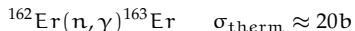


^{163}Ho production and chemical purification



Production

^{163}Ho production from ^{162}Er neutron activation



- ^{162}Er irradiation at ILL nuclear reactor @ Grenoble: high thermal n flux
- cross section burn up $^{163}\text{Ho}(n, \gamma)^{164}\text{Ho}$ not negligible ($\sim 200\text{b}$)
- $^{165}\text{Ho}(n, \gamma)^{166\text{m}}\text{Ho}$ ($\beta, \tau_{1/2} \sim 1200\text{y}$) from Ho contamination or ^{164}Er

Tm 163 1.81 h	Tm 164 5.1 m, 2.0 m	Tm 165 30.06 h	Tm 166 7.70 h	Tm 167 9.25 d	Tm 168 93.1 d
Er 162 0.139	Er 163 75 m	Er 164 1.601	Er 165 10.3 h	Er 166 33.503	Er 167 2.3 s, 22.869
Ho 161 6.7 s, 2.5 h	Ho 162 68 m, 15 m	Ho 163 1.1 s, 4570 a	Ho 164 37 m, 29 m	Ho 165 100	Ho 166 1200 a, 26.80 h
Dy 160 2.329	Dy 161 18.889	Dy 162 25.475	Dy 163 24.896	Dy 164 28.260	Dy 165 1.3 m, 2.35 h
Tb 159 100	Tb 160 72.3 d	Tb 161 8.00 d	Tb 162 7.76 m	Tb 163 18.5 m	Tb 164 9.0 m

Purification

Chemical purification @ PSI before and after the irradiation

- radiochemical separation with ion-exchange chromatography
- efficiency better than 79%
- Expected $^{166\text{m}}\text{Ho}$ contamination fraction: $\sim 10^{-3}$

Sample processed

Enriched Er_2O_3 samples irradiated @ ILL, pre and post processed @ PSI:

- 25 mg, 55 days irradiation, $A(^{163}\text{Ho}) \sim 5\text{MBq}$
- 150 mg, 53 days irradiation, $A(^{163}\text{Ho}) \sim 38\text{MBq}$
- 544 mg, 50 days irradiation, $A(^{163}\text{Ho}) \sim 120\text{MBq}$
- * $\sim 100\text{MBq}$ enough for R&D and 500 pixels



Ion implanter designed to embed Ho inside the detectors absorbers and to perform a mass separation of the ^{163}Ho from the other contaminants.

- extraction voltage 30-50 kV \rightarrow 10-100 nm implant depth
- $^{163}\text{Ho}/^{166\text{m}}\text{Ho}$ separation better than 10^5

Au co-evaporation:

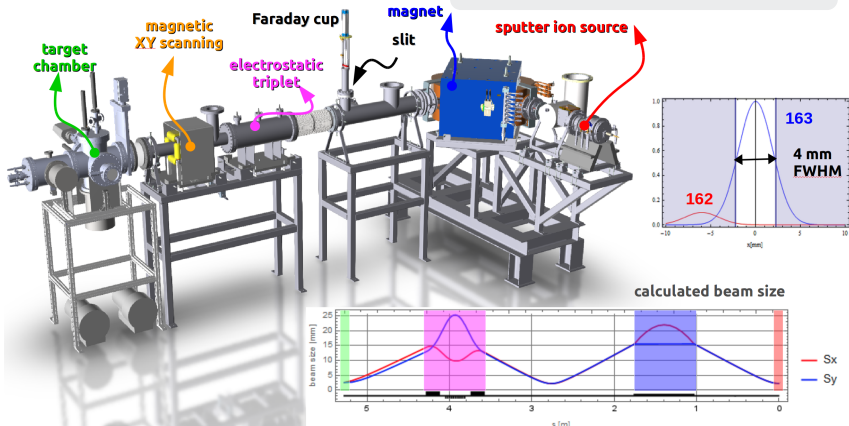
- to fully encapsulate the source
- to compensate the saturation of the ^{163}Ho concentration in the absorber
- to avoid oxidation
- heat capacity

Target chamber:

- 4 COMIC microwave sources
 - 4 Ar beams hit on 4 Au targets
- \rightarrow 4 in order to increase the deposition rate and uniformity

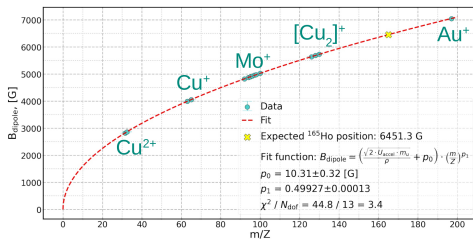
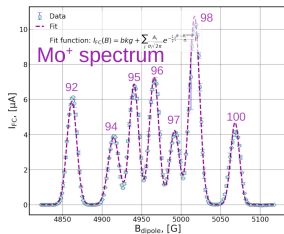
Main components:

- Ar penning sputter ion source
- magnetic dipole mass analyzer ($B_{\text{max}} = 1 \text{ T}$)
- faraday cup and slit
- target chamber for Au co-evaporation

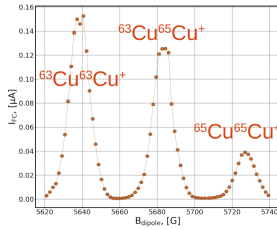
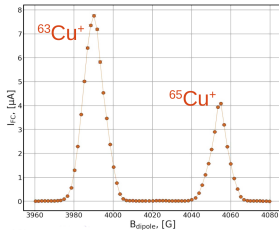
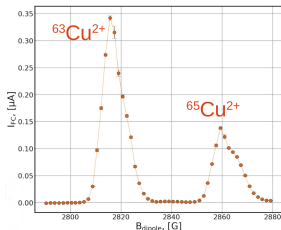




Magnetic field vs mass-to-charge ratio calibration with Cu, Au and Mo peaks.



- Cu/Au from sputter target/holder
- Mo from the anode
- The source produces also multiple-ionized and dimeric ions from the same material, which can also be used for calibration



for more details

Maria Fedkevych's talk @ NuMass 2022

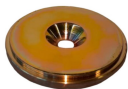


Efforts are put to build the most suitable target for the Ho sputtering

→ different techniques for target fabrication are tested

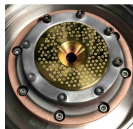
Molecular plating

Electrodeposition of Ho complexes in an organic solvent at high voltages with high uniformity and efficiency (>90%)



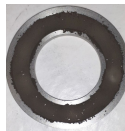
Drop-on-demand inkjet printing

put droplets of solution containing compound and let solvent evaporate to deposit the dissolved compound



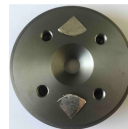
Sintered targets

$\text{Ho}(\text{NO}_3)_3$ in a metallic mixture of Zr and Y fine-grained powder prepared pressed at 350 bar/cm² and baked at 950°C

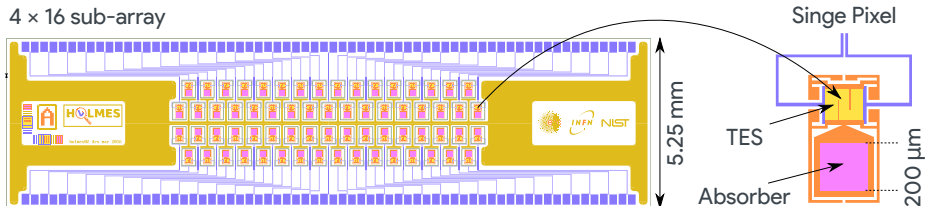


Coupled reduction

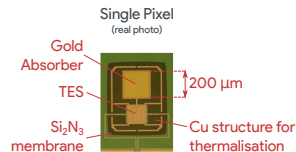
Ho reduction and diffusion into backing material due to thermodynamically favourable formation of intermetallic compound



With **sintered target** we obtained the best current-stability: O(200) nA over 15 h!



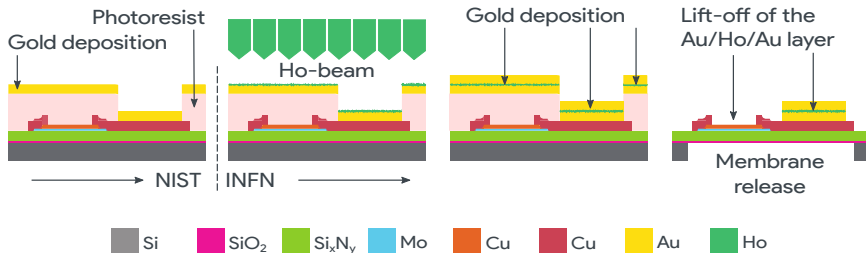
- Mo/Cu TES coupled to Gold absorbers where ^{163}Ho will be ion-implanted
- $2\ \mu\text{m}$ Gold thickness for full e/γ absorption
- Side-car design to avoid TES proximitation effect
- Thermal conductance G engineering for τ_{decay} control
- 4×16 linear sub-array designed for high implant efficiency and low parasitic L
- **Optimized design for high speed and high resolution:**



Specs @ 2.8 keV : $\Delta E_{\text{FWHM}} \simeq 3 - 4\ \text{eV}$, $\tau_{\text{rise}} \simeq 10\ \mu\text{s}$, $\tau_{\text{decay}} \simeq 100\ \mu\text{s}$



^{163}Ho isotopes embedded in metallic absorbers (through ion-implantation)



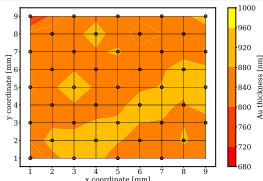
- Fabrication in two steps:
 - ▶ NIST: TES fabrication with 1 μm Au absorber
 - ▶ INFN: ^{163}Ho implantation, final deposition of 1 μm Au and SiN membrane release
- final micromachining step definition in progress
 - ⇒ KOH vs DRIE machining



Au deposition

1 μm of Au deposited

- with Ion beam sputter system
- at rate of around 52 nm/h
→ about 20 h for 1 μm
- gold thickness uniformity
→ $\sigma_t/t \sim 4\%$



Lift-off

Removal of the resist mask (7 μm thickness)

- sample in acetone at 40°C for 24 h

After the lift-off, the Au deposited remains only on the absorber:

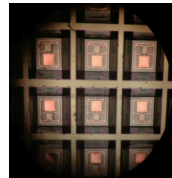
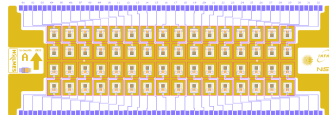
→ Minimal crowning and almost isotropical deposition thanks to the 4 ion beam sources



Membrane release

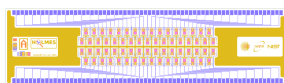
KOH

- Anisotropic wet etching
- Requires more spacing between pixels
- Successfully tested

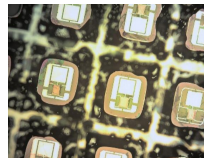


DRIE

- Silicon Deep Reactive Ion Etching
- Best for close packing
- High implant efficiency
- Not yet tuned

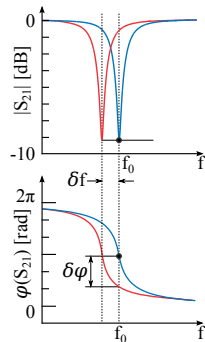
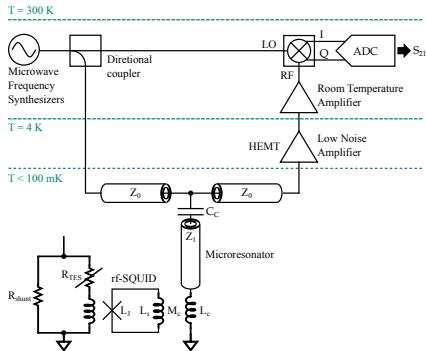


calculated photo beam FWHM width



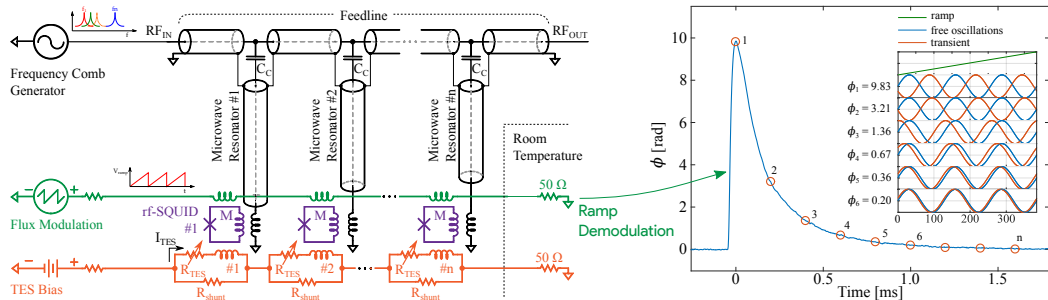


HOLMES TESs readout is based on microwave rf-SQUID multiplexing



- rf-SQUID inductively coupled to a dc-biased TES and to a high-Q superconducting $\lambda/4$ -wave resonator
- Change in TES current \Rightarrow change in the input flux to the SQUID
- The rf-SQUID transduces a change in input flux into a variation of resonant frequency and phase
- Each micro-resonator can be continuously monitored by a probe tone

Microwave rf-SQUID multiplexing (cont.)

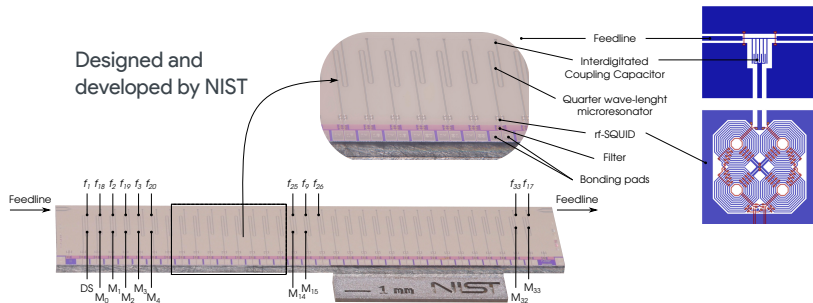


- By coupling many resonators to a single microwave feedline it is possible to readout multiple detectors
- Sensors are monitored by a set of sinusoidal probe tones (frequency comb)
- At equilibrium, the resonator frequencies are matched to the probe tone frequencies, and so each resonator acts as a short to ground
- The ramp induces a controlled flux variation in the rf-SQUID, which is crucial for linearizing the response
- Large multiplexing factor (> 100) and bandwidth, **currently limited by the digitizer bandwidth**

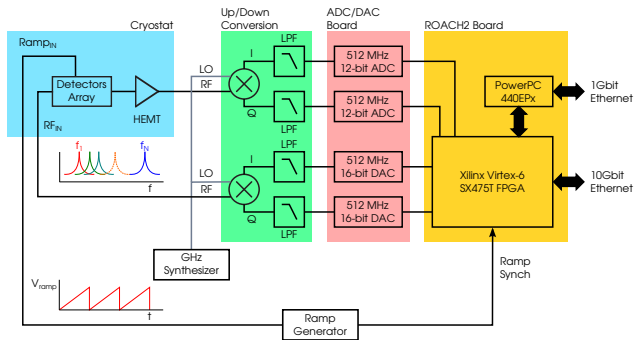
The Multiplexing chip



The core of the microwave multiplexing is the **multiplexer chip**



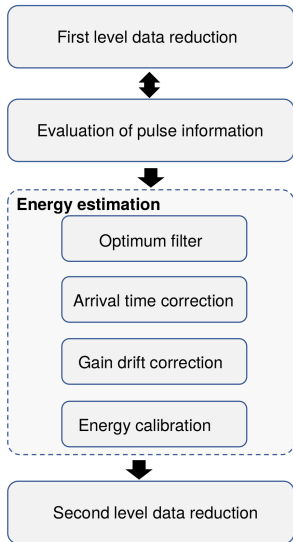
- Superconducting 33 quarter-wave coplanar waveguide (CPW) microwave resonators covering 500 MHz in the 4-8 GHz frequency range
- 200 nm thick Nb film deposited on high-resistivity silicon ($\rho > 10 \text{ k}\Omega \cdot \text{cm}$)
- each resonator has a trombone-like shape with slightly different length
- 2 MHz bandwidth per resonator
- separation between resonances 14 MHz (to prevent cross-talk)
- resonance depth greater than 10 dB
- squid equivalent noise less than $2\mu\phi_0 / \sqrt{\text{Hz}}$



- Software Defined Radio with the open system ROACH2 (Casper collaboration)
- ADC BW 550 MHz
- real time pulse reconstruction
→ at the moment readout available for 64 channels

Multiplexing factor proportional to the target rise time

- $n_{TES} \approx 3.4 \cdot \tau_{rise}$
- requiring $\tau_{rise} = 10\mu s$



- Robust analysis is mandatory for achieving the expected microcalorimeter intrinsic energy resolution.
- The data from each pixel need to be processed separately.

Watson toolkit

- Software for low temperature detector data analysis
- Object oriented programming. Written in python (numpy and scipy)
- Fast, easy to read, easy to fix code
- GUI with QT5 for handy day to day operations
- Data are stored in hdf5 (hierarchical, filesystem-like data format)

```
#!/usr/bin/env python3
import sys
import numpy as np
import scipy as sp
import h5py
import matplotlib.pyplot as plt
import os
import time
import logging
import argparse
import glob
import shutil
import subprocess
import signal
import sys

def main():
    parser = argparse.ArgumentParser()
    parser.add_argument('--input', type=str, required=True, help='Input file path')
    parser.add_argument('--output', type=str, required=True, help='Output file path')
    parser.add_argument('--verbose', type=bool, default=False, help='Verbose mode')
    parser.add_argument('--help', type=bool, default=False, help='Show help message')
    args = parser.parse_args()

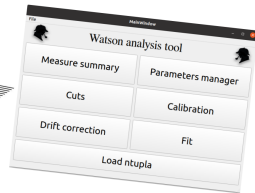
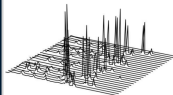
    if args.help:
        parser.print_help()
        return

    if args.verbose:
        logging.basicConfig(level=logging.INFO)

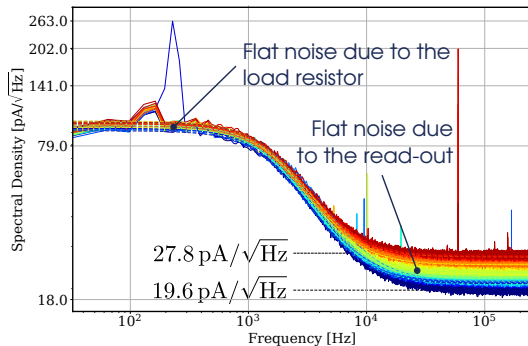
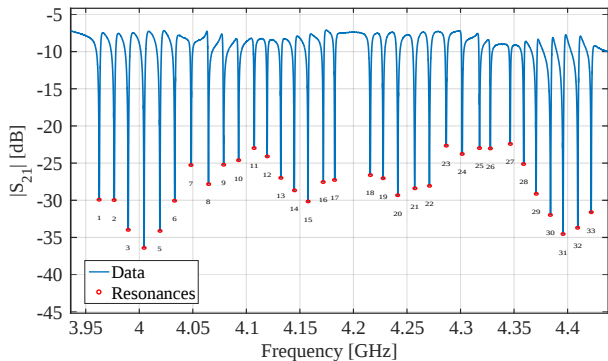
    # Load data
    data = h5py.File(args.input, 'r')
    # ... (rest of the code) ...
    data.close()

    # Save results
    results = h5py.File(args.output, 'w')
    # ... (rest of the code) ...
    results.close()

if __name__ == '__main__':
    main()
```



Multiplexing: characterization results



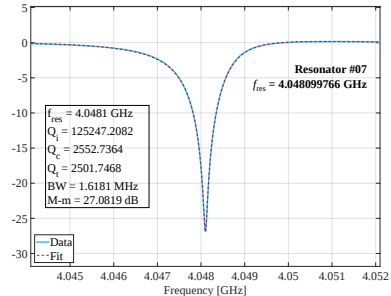
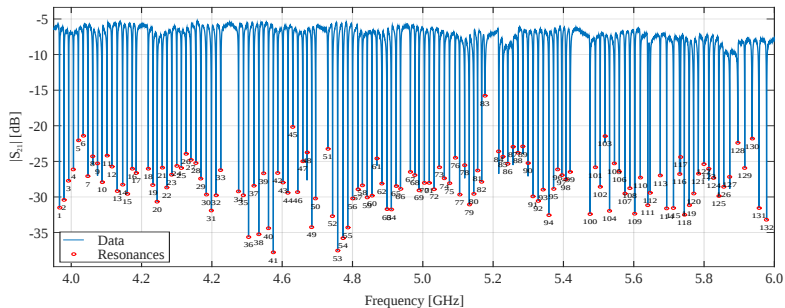
		Required	Measured
Resonators bandwidth	Δf_{BW} [MHz]	2	2 ± 1
Resonators spacing	Δf [MHz]	14	14 ± 1
Resonators depth	ΔS [dB]	> 10	29 ± 6

All the microresonator parameters match the HOLMES specification

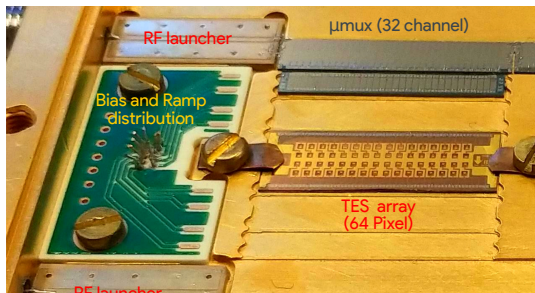
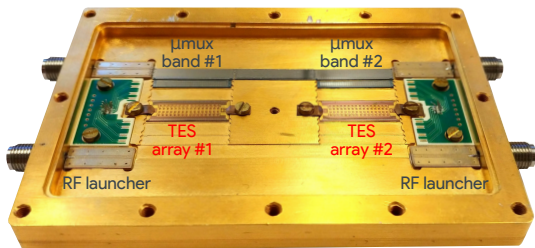
Improved read out noise
 $\rightarrow n_s = (23 \pm 2) \text{ pA} / \sqrt{\text{Hz}}$
 Previous work
 $\rightarrow n_s = (26 \pm 7) \text{ pA} / \sqrt{\text{Hz}}$
 more details on
 IEEE TAS 31 (2021) 5, 2100205



Forward transmission S_{21} of 4 different band chips wired in series and an example of resonance fit



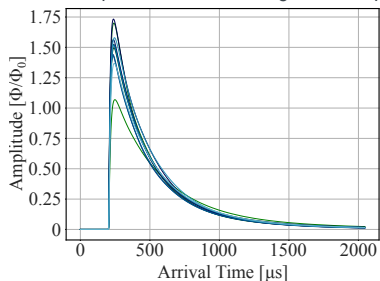
Four μ mux in series are able to cover a wide frequency range from 4 to 6 GHz



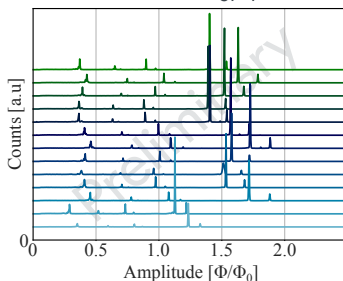
- Holder designed to host 128 Channels:
 - ▶ $2 \times (4 \times 16)$ sub arrays
 - ▶ $4 \times \mu\text{mux}$ multiplexer chips with 4 bands
- 8 holders will cover the entire HOLMES in its final configuration (1024 channels);
- Preliminary low temperature tests performed with **fully processed arrays** (with KOH):
 - ▶ detector with (1 μm) absorber at NIST
 - ▶ absorber finalized (1 μm) at MIB
 - ▶ wet etching at MIB
- **32+32 TES pixels bonded** (half of the available)
- Absorbers without the ^{163}Ho implanted
- New SDR firmwares for 16 and 32 channels:
 - 16-channel version fully operational
 - 32-channel version under testing
- New up/down-conversion system fully operational



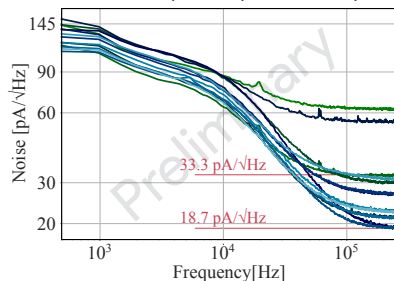
Event pulses due to the Manganese x-rays



Uncalibrated energy spectra



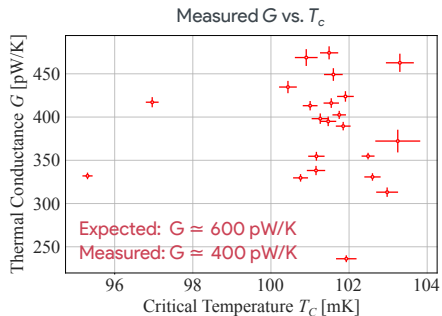
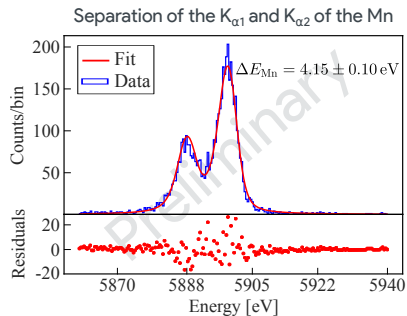
Noise Amplitude Spectral Density



- **non implanted detectors** with KOH membrane release
- 13/16 working detectors (3 detectors with problematic resonators)
- Calibration run performed with a primary ^{55}Fe source faced to different targets
- X-ray fluorescence emission lines:
 - ^{55}Mn (5.9 keV) ^{40}Ca (3.7 keV) ^{40}Cl (2.6 keV) ^{27}Al (1.5 keV)

Measured read out noise
 $n_s \sim (19 - 33) \text{ pA}/\sqrt{\text{Hz}}$

- Compatible with the previous prototypes
[Eur. Phys. J. C \(2019\) 79:304](#)
- Two channels with higher noise due to not optimal rf-SQUID oscillations



For the best detector: $\Delta E_{Mn} = 4.15 \pm 0.10 \text{ eV @ } 5.9 \text{ keV}$

- Energy resolution in the (4 - 6) eV range @5.9 keV
Large spread probably due to the large G dispersion
different $G \Rightarrow$ different working point
- $\tau_{\text{rise}} \simeq 20 \mu\text{s}$ and $\tau_{\text{fall}} \simeq 300 \mu\text{s}$
longer fall time due to lower thermal conductance G

KOH vs DRIE machining

- same energy resolution and rise time
- longer decay time and larger coupling dispersion



The count rate at the ROI is very low (0.26 counts/eV/day/det @ [2650,2833]eV)

→ the fraction of background signals must be kept as low as possible

Background

1. Pile-up

→ the main background source for pixel with $A_{EC} \sim 300$ Bq and $\tau_R \sim 1.5$ μ s. (0.8 counts/eV/day/det @ ROI)

2. Internal radionuclides

^{166m}Ho → expected count rate < 0.01 counts/eV/day/det @ ROI

3. Natural radioactivity

Smooth and almost flat background @ ROI except for ^{40}K

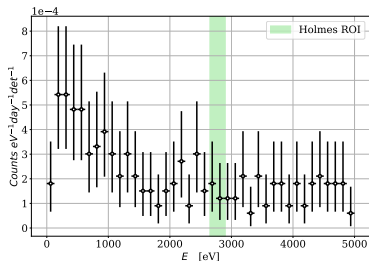
4. Cosmic rays

GEANT 4 simulation 5×10^{-5} counts/eV/day/det @ [0,4000] eV

3. and 4. can be comparable or even overcome the pile-up rate if the ^{163}Ho activity per pixel is too low.

Background measurement

Single interaction in a pixel produces a background spectrum which seems to be monotonically decreasing.



0.0001 counts/eV/day/det @ HOLMES ROI

→ lowering with a muon veto



- A powerful tool to determine the effective electron-neutrino mass is the calorimetric measurement of the energy released in ^{163}Ho electron capture (EC)
- The HOLMES experiment will perform a direct measurement of the neutrino mass by using microcalorimeters with absorber ^{163}Ho -implanted
- Ion implanter is working as expected. The production of a proper sputter target is almost ready!
- The software for analysis and signal processing of microcalorimeters events is up and running!
- For reading out the 1024 detectors, HOLMES will use the microwave multiplexing read-out
 - All the microresonator parameters match the HOLMES specification
- Transition edge sensors with Au absorber where the ^{163}Ho will be ion-implanted
 - Tested and tuned the final array fabrication processes
 - TES characterization with a fluorescence source without Ho
 - The performances (energy and time resolution) required by HOLMES are achieved
- The first phase of the HOLMES experiment is expected on the last quarter of 2022: a low dose implantation of a 2x32 pixel array